Available online at www.sciencedirect.com
SCIENCE DIRECT®
International Journal of Mass Spectrometry 228 (2003) 497–506
International Journal of Mass Spectrometry
www.elsevier.com/locate/ijms

A theoretical study of the ground and excited states of the $CHCl^{2+}$ dication and the $CHCl^{+}$ cation

Jana Roithová, Jan Hrušák, Zdenek Herman*

V. Èermák Laboratory, J. Heyrovský Institute of Physical Chemistry, Academy of Sciences of the Czech Republic, Dolejškova 3, CZ-182 23 Prague 8, Czech Republic

Received 29 November 2002; accepted 19 March 2003

Dedicated to Professor Helmut Schwarz on the occasion of his 60th birthday in appreciation of his manifold contributions to mass spectrometry and ion chemistry.

Abstract

Ground and excited states of the dication $CHCl^{2+}$ and the corresponding cation $CHCl^{+}$ were investigated using the CASSCF-AQCC method with moderate ANO basis sets. Both isomers of the dication and cation were investigated: $HCCl^{2+}$ and $HCCl^{+}$ (with H bonded to C), and $CClH^{2+}$ and $CClH^{+}$ (with H bonded to Cl). The energetics and geometries of stable configurations were characterized and energies of both adiabatic and vertical transitions between the dication and the cation were determined. The data were found essential to interpret correctly experimental results on charge transfer collision of the dication with noble gases and to assess the role of the $CClH^{+}$ isomer in them.

Keywords: Dications; Ground and excited states; Ionization energy (IE); AQCC

1. Introduction

Multiply charged molecular ions have been know in mass spectrometry for a long time [1–3]. Quite recently, multiply charged and multi-protonated large molecules and biomolecules, produced by special ionization methods, have been a basis for mass spectrometric analysis of these species [4].

In the 1980s, considerable attention of both experimentalists and theoreticians was devoted to the formation, stability, and structure of organic multiply charged molecular ions in their ground electronic states [5–8]. During the last decade, chemical reactions of molecular dications have been observed and studied [9–13]. Detailed studies of the dynamics of collision processes of multiply charged ions require a good knowledge of not only the ground state, but also of electronically excited states and often their spectroscopic properties. Theoretical and experimental efforts have resulted in increasing amount of reliable information on small molecular dications like CO^{2+} [14], $CO_2{}^{2+}$ [15], etc., mainly formed in double-ionization processes from neutral molecules. Much less is known, however, on molecular dications formed as fragments in dissociative double-ionization [16–19].

This paper reports on quantum chemical calculations of the dication $CHCl^{2+}$. Our interest in this dication stems from our recent experimental studies of

* Corresponding author. Tel.: +420-2-6605-3514; fax: +420-2-8658-2307.
E-mail address: Zdenek.herman@jh-inst.cas.cz (Z. Herman).

1387-3806/$ – see front matter
doi:10.1016/S1387-3806(03)00141-6

its behavior in collisions with D_2 [20,21] and noble gases Ar, Kr, and Xe [21,22]. Both charge transfer processes resulting in formation of a pair of singly charged ions, and chemical reactions, including proton transfer to D_2 and Ar, were observed. The translational energy spectrum of $CHCl^+$ from the charge transfer of $CHCl^{2+}$ with Ar possesses three peaks in the reaction exoergicity of an energy release of 2.0, 2.9, and 3.8 eV [22]. In order to interpret this energy release, reliable information on both ground and excited states of the dication $CHCl^{2+}$ and of the corresponding cation $CHCl^+$ was needed.

Previous calculations on the dication $CHCl^{2+}$ form a part of the ab initio theoretical study of the chloromethane dication fragmentation [23]. The dication $HCCl^{2+}$ was found to exhibit a minimum on the potential energy surface (PES) of the $^1\Sigma$ state with ionization energy IE($HCCl^+$) of 17.2 eV (CASSCF/TZP). Vertical and adiabatic ionization energies of $HCCl^+$ were also estimated [6] on the MP4/6-31G**//MP2/6-31G* level giving 17.8 and 17.0 eV, respectively. The $CHCl^{2+}$ dication can be produced by double-ionization of CH_3Cl. The dication CH_3Cl^{2+} is not stable and decomposes to give $CHCl^{2+}$ [24].

2. Computational details

A modification of the configuration–interaction method namely the averaged quadratic coupled cluster (AQCC) method was applied in these calculations. The method describes well excitation energies [25]. Recently, the AQCC method has been found to reproduce the electronic properties of the $^1B_1$ excited state of SO_2 [26] with a rather high accuracy. In addition, applications to the excited states of CF_2^{2+} [17] demonstrated the power of this approach. Furthermore, this method is approximately size-consistent and slightly superior to the traditional MR-CI.

Full valence reference space was employed in the complete active space self-consistent field (CASSCF-AQCC) [27,28]. Details of the calculations, and the basis set dependencies are discussed in Section 3. The following atomic natural orbital (ANO) basis set [29] in the general contraction (17s12p5d4f/7s6p3d2f) for chlorine, (14s9p4d3f/5s4p2d1f) for carbon, and (8s4p3d/4s3p2d) for hydrogen was used. This resulting basis set is denoted as ANO-I. The justification of this contraction was checked by a test calculation: in addition to the ANO-I basis set also a non-contracted basis set (ANO-II) was used. All the calculations were performed with MOLPRO 98 program [30].

3. Results and discussion

3.1. Test calculations

In general, the CAS-AQCC method is computationally very demanding. Since the effect of references in the AQCC expansion with low weights is expected to be small, it was decided to select the major components only. Two different reference selections were tested. The first selection of references consisted of all individual configurations in the CAS wave function with weights larger than 0.05 ($k > 0.05$) and the second selection used all configurations with weights larger than 0.01 ($k > 0.01$). Similarly, the influence of the basis set contraction on the basis sets ANO-I and ANO-II was tested. The vertical excitation energy of $HCCl^{2+}$ ($R_{C–H} = 1.128$ Å, $R_{C–Cl} = 1.474$ Å, $\alpha_{H–C–Cl} = 180^\circ$) was taken as an indicator of the influence of the size of the reference space and of the basis set (Table 1).

Increasing the basis from the contracted (ANO-I) to the non-contracted Roos' basis set (ANO-II) did not result in any considerable improvement of the relative energies (the maximum change of the excitation energy was 0.02 eV). However, the effect of increasing the reference space was about 5–10 times stronger: in the case of $CHCl^{2+}(^3A_2)$ it was 0.21 eV. As the result, the contracted basis set (ANO-I) and the bigger configuration space ($k > 0.01$) was used in the calculations. Such calculations resulted in about 50–70 references.

3.2. Equilibrium structures

The calculations were performed under the restriction of the C_s symmetry. For linear structures, the

Table 1
Test calculations geometry: $HCCl^{2+}$ ($R_{C–H} = 1.128$ Å, $R_{C–Cl} = 1.474$ Å, $\alpha_{H–C–Cl} = 180°$)

$CHCl^{2+}$	$k > 0.01$, ANO-II (ΔE, eV)	$k > 0.01$, ANO-I (ΔE, eV)	$k > 0.05$, ANO-II (ΔE, eV)	$k > 0.05$, ANO-I (ΔE, eV)
$^1A_1$	0.00	0.00	0.00	0.00
$^3A_1$	−5.23	−5.24	−5.24	−5.25
$^3A_1$	−5.92	−5.93	−5.95	−5.96
$^3A_2$	−5.93	−5.94	−6.12	−6.13
$^1A_2$	−6.55	−6.56	−6.49	−6.51
$^1A_1$	−6.66	−6.68	−6.75	−6.76

C_{2v} symmetry constrains were applied. For simplicity, Mulliken symbols are used for both bent and linear structures rather than spectroscopic symbols. Consequently, S_0, S_1, T_1, T_2 are used for a more explicit identification of the singlet ground state, first singlet excited state, and first and second triplet excited state, respectively, rather than X, A, B, C, etc. For the dication $CHCl^{2+}$ two stable isomers, H–C–Cl^{2+} and C–Cl–H^{2+}, with H bonded either to C or Cl atom, were taken into account. For the isomer C–Cl–H^{2+}, the designation iS_0, iS_1, iT_1, iT_2 is used. Similarly, for the ground and excited states of the $HCCl^+$ ($CClH^+$) cation the designation D_0, D_1 (iD_0, iD_1) has been used for doublets and Q_1, Q_2 (iQ_1, iQ_2) for quartets, respectively.

The optimized geometrical parameters, total energies (in hartree) and leading configurations for all optimized structures are listed in Table 2. In addition, the total energies are recalculated in electron volts and related to the ground state D_0 of $HCCl^+$ (E_{rel} in Table 2). The energy level diagram is shown in Fig. 1.

3.2.1. H–C–Cl^{2+} and H–C–Cl^+

The optimized geometries lead to eight states of the dication H–C–Cl^{2+}. The ground state ($S_0\{^1A_1\}$) is linear, all the excited states ($S_1\{^1A''\}$, $S_2\{^1A'\}$, $S_3\{^1A''\}$, $T_1\{^3A'\}$, $T_2\{^3A''\}$, $T_3\{^3A'\}$, $T_4\{^3A''\}$) have bent geometries. In the case of $S_3\{^1A''\}$, the root-flipping problem was encountered, and therefore, the state-average wave function was used.

The dication H–C–Cl^{2+} in its ground state has a very short C–Cl bond (1.474 Å). This indicates an efficient overlap of the bonding orbitals leading to the stabilization of the structure (the most stable structure of all dications $CHCl^{2+}$). The first excited singlet state S_1 lies at 4.85 eV above it, and the first and second excited triplet states (T_1 and T_2) are 4.13 and 4.57 eV above it, respectively (see Fig. 1). This big energy gap between the ground state and the first excited state is typical for closed-shell systems. The C–Cl bond in the excited states S_1, T_1, and T_2 states is substantially longer (1.710, 1.776, and 1.814 Å, respectively) than in the ground state (1.474 Å). This is caused by an

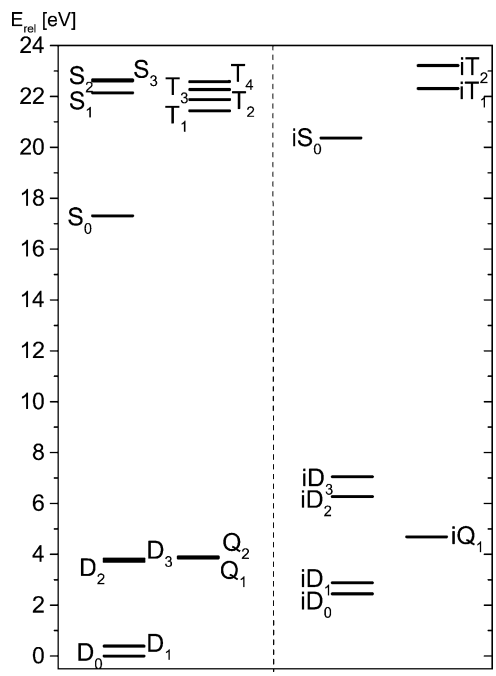

Fig. 1. Energy diagram (total energies of optimized structures related to the ground state D_0 of $HCCl^+$ and recalculated in electron volts, i.e., E_{rel} in Table 2).

Table 2
Optimized geometries, energies, relative energies and leading configurations (AQCC/cc-pVTZ) of $HCCl^+$, $HCCl^{2+}$, $CClH^+$, and $CClH^{2+}$

	State	Leading configurations	Energy		Structure		
			E_{tot} (hartree)	E_{rel} (eV)	$R_{C–Cl}$ (Å)	$R_{C–H}$ (Å)	$\alpha_{H–C–Cl}$ (°)
$HCCl^+$	$D_0\{^2A'\}$	0.927 $\|1a'^2 2a'^2 3a'^2 4a'^2 1a''^2 5a'^1\|$	−497.901802	0	1.554	1.093	132.6
	$D_1\{^2A''$	0.927 $\|1a'^2 2a'^2 3a'^2 1a''^2 4a'^2 2a''^1\|$	−497.887616	0.39	1.534	1.082	180.0
	$D_2\{^2A'\}$	0.831 $\|1a'^2 2a'^2 3a'^2 4a'^1 1a''^2 5a'^2\|$	−497.764663	3.73	1.896	1.110	100.1
		0.208 $\|1a'^2 2a'^2 3a'^2 4a'^2 1a''^1 5a'^1 2a''^1\|$					
	$D_3\{^2A''\}$	0.864 $\|1a'^2 2a'^2 3a'^2 4a'^2 1a''^1 5a'^2\|$	*−497.761392*	3.82	1.997	1.115	97.6
		0.239 $\|1a'^2 2a'^2 3a'^2 4a'^2 1a''^2 2a''^1\|$					
	$Q_1\{^4A''\}$	0.939 $\|1a'^2 2a'^2 3a'^2 1a''^2 4a'^1 5a'^1 2a''^1\|$	−497.758499	3.86	1.797	1.090	117.0
	$Q_2\{^4A'\}$	0.938 $\|1a'^2 2a'^2 3a'^2 4a'^2 1a''^1 5a'^1 2a''^1\|$	−497.759969	3.90	1.829	1.089	120.6
$HCCl^{2+}$	$S_0\{^1A_1\}$	0.923 $\|1a_1^2 2a_1^2 3a_1^2 1b_1^2 1b_2^2\|$	−497.265801	17.31	1.474	1.128	180.0
	$T_1\{^3A'\}$	0.930 $\|1a'^2 2a'^2 3a'^2 1a''^2 4a'^1 5a'^1\|$	−497.114007	21.44	1.710	1.127	126.1
	$T_2\{^3A''\}$	0.934 $\|1a'^2 2a'^2 3a'^2 4a'^2 1a''^1 5a'^1\|$	−497.097841	21.88	1.776	1.130	128.8
	$S_1\{^1A''\}$	0.936 $\|1a'^2 2a'^2 3a'^2 4a'^2 1a''^1 5a'^1\|$	−497.087457	22.16	1.814	1.134	129.0
	$T_3\{^3A'\}$	0.927 $\|1a'^2 2a'^2 3a'^2 1a''^1 4a'^2 2a''^1\|$	−497.083155	22.28	1.709	1.132	168.0
		0.589 $\|1a'^2 2a'^2 3a'^2 1a''^2 4a'^1 5a'^1\|$					
	$T_4\{^3A''\}$	0.744 $\|1a'^2 2a'^2 3a'^2 1a''^2 4a'^1 2a''^1\|$	−497.071296	22.60	1.746	1.135	169.9
		0.567 $\|1a'^2 2a'^2 3a'^2 1a''^1 4a'^2 5a'^1\|$					
	$S_2\{^1A'\}$	0.652 $\|1a'^2 2a'^2 3a'^2 1a''^2 4a'^1 5a'^1\|$	−197.070419	22.62	1.778	1.136	159.8
		0.619 $\|1a'^2 2a'^2 3a'^2 1a''^1 4a'^2 2a''^1\|$					
	$S_3\{^1A''\}$	0.708 $\|1a'^2 2a'^2 3a'^2 1a''^2 4a'^1 2a''^1\|$	*−197.069493*	22.65	1.774	1.136	175.3
		0.611 $\|1a'^2 2a'^2 3a'^2 1a''^1 4a'^2 5a'^1\|$					
					$R_{C–Cl}$ (Å)	$R_{Cl–H}$ (Å)	$\alpha_{H–C–Cl}$ (°)
$CClH^+$	$iD_0\{^2A'\}$	0.921 $\|1a'^2 2a'^2 3a'^2 1a''^2 4a'^2 5a'^1\|$	−497.811807	2.45	1.817	1.308	100.8
	$iD_1\{^2A''\}$	0.920 $\|1a'^2 2a'^2 3a'^2 1a''^2 4a'^2 2a''^1\|$	−497.795871	2.88	1.963	1.304	93.4
	$iQ_1\{^4A''\}$	0.943 $\|1a'^2 2a'^2 3a'^2 1a''^2 4a'^1 5a'^1 2a''^1\|$	−497.729618	4.69	1.706	1.300	100.3
	$iD_2\{^2A'\}$	0.898 $\|1a'^2 2a'^2 3a'^2 1a''^2 4a'^1 5a'^2\|$	−497.671489	6.27	1.534	1.413	112.7
	$iD_3\{^2A''\}$	0.713 $\|1a'^2 2a'^2 3a'^2 1a''^2 4a'^1 5a'^1 2a''^1\|$	−497.640425	7.11	1.639	1.345	104.4
		0.463 $\|1a'^2 2a'^2 3a'^2 1a''^2 4a'^2 2a''^1\|$					
		0.328 $\|1a'^2 2a'^2 3a'^2 1a''^2 5a'^2 2a''^1\|$					
$CClH^{2+}$	$iS_0\{^1A'\}$	0.909 $\|1a'^2 2a'^2 3a'^2 4a'^2 1a''^2\|$	−497.153369	20.37	1.741	1.378	95.0
	$iT_1\{^3A'\}$	0.931 $\|1a'^2 2a'^2 3a'^2 1a''^2 4a'^1 5a'^1\|$	−497.081843	22.31	1.625	1.374	100.8
	$iT_2\{^3A''\}$	0.936 $\|1a'^2 2a'^2 3a'^2 4a'^1 1a''^2 2a''^1\|$	−497.049292	23.20	1.760	1.370	93.8

All relative energies refer to the ground state of $HCCl^+$ cation (D_0). State-averaged wave function are in italics.

excitation of the bonding electron to the non-bonding orbital located on carbon and leads to bent structures with the H–C–Cl angles of 126.1, 128.8, and 129.0° for the states S_1, T_1, and T_2, respectively.

Potential energy profiles of the ground state S_0 and of the excited states S_1, T_1, and T_2 (optimized structures) along the C–Cl bond are shown in Fig. 2. An extension of this bond leads to experimentally observed dissociation fragments CH^+ and Cl^+ [21]. Fig. 3 shows the respective potential energy profiles for optimized structures S_0, S_1, T_1, and T_2 along the C–H bond dissociation. A change of slope of the curves at internuclear separations longer than 2.5 Å is caused by a crossing of the attractive curve of the interaction between H and CCl^{2+} with the repulsive curve of Coulomb interaction between H^+ and CCl^+.

The excited states T_3, T_4, S_2, and S_3 result from double excitation. Their equilibrium structures exhibit a general trend with long C–Cl bond and a bond angle in the range of 160–175°.

The geometry of the corresponding cation H–C–Cl^+ was optimized for six different states ($D_0\{^2A'\}$,

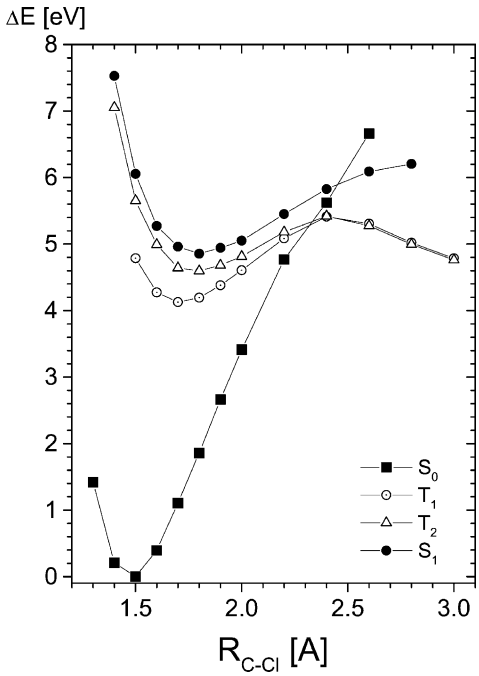

Fig. 2. Potential energy curves of S_0, S_1, T_1, T_2 states along the constrained C–Cl bond.

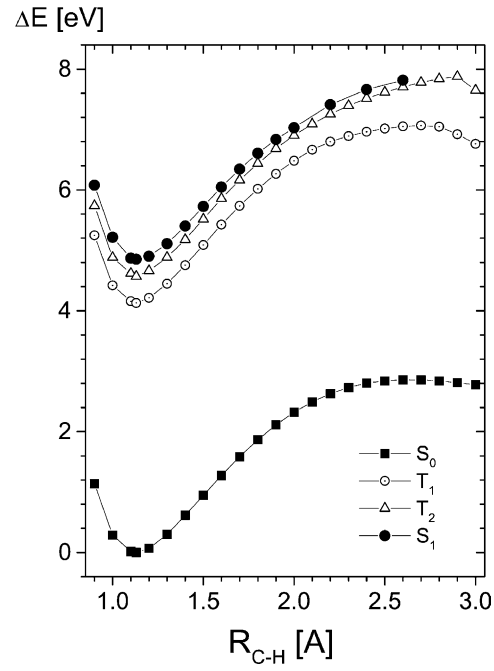

Fig. 3. Potential energy curves of S_0, S_1, T_1, T_2 states along the constrained C–H bond.

$iD_1\{^2A''\}$, $D_2\{^2A'\}$, $D_3\{^2A''\}$, $Q_1\{^4A'\}$, and $Q_2\{^4A''\}$). The ground state $^2A'\}$ has a bent geometry, because the unpaired electron fills the non-bonding orbital on carbon, located in the plane of all three atoms. The length of the C–Cl bond is 1.55 Å. The first excited state $D_1\{^2A''\}$ has the unpaired electron in the orbital perpendicular to the H–C–Cl plane and has the linear geometry. This represents an example of the Renner–Teller effect: the degenerate linear $^2\Pi$ state splits into two states, a linear one ($^2A''$) and a bent one ($^2A'$). The situation is schematically shown in Fig. 4. Contrary to the dication, the energy gap between the ground state D_0 and the first excited state D_1 of the cation is only 0.39 eV (see the difference between minima in Fig. 4). The excited states D_2 and D_3 originate from an excitation of the bonding (C–Cl) electron to the orbital on carbon containing the unpaired electron. This increases the repulsion on carbon and results in a decrease of the bonding angle to 100.1 and 97.6°, respectively, while the C–Cl bond extends to 1.9 and 2.0 Å, respectively. The quartets have three unpaired electrons: in addition to the original unpaired electron, two other electrons come from splitting the bonding electron pair on the C–Cl bond: one electron is excited to the non-bonding orbital. This leads to an increase of the C–Cl distance to approximately 1.8 Å.

3.2.2. C–Cl–H^{2+} and C–Cl–H^+

The C–Cl–H^{2+} dication (H bonded to Cl) represents another stable isomer of $CHCl^{2+}$. Optimization of its geometry leads to three states ($iS_0\{^1A'\}$, $iT_1\{^3A'\}$, and $iT_1\{^3A''\}$). The singlet state $iS_1\{^1A''\}$ is dissociative. (As stated earlier, for a better orientation, we use the notation iS for singlets and iT for triplets of the isomer C–Cl–H^+, instead of the usual S(T) notification assigned to the isomer H–C–Cl.) The C–Cl bond in both the ground state iS_0 and the excited states iT_1 and iT_2 of C–Cl–H^{2+} is longer than in the isomer H–C–Cl^{2+}, because of lack of a multiple bond character. On the contrary, two lone pairs of electrons

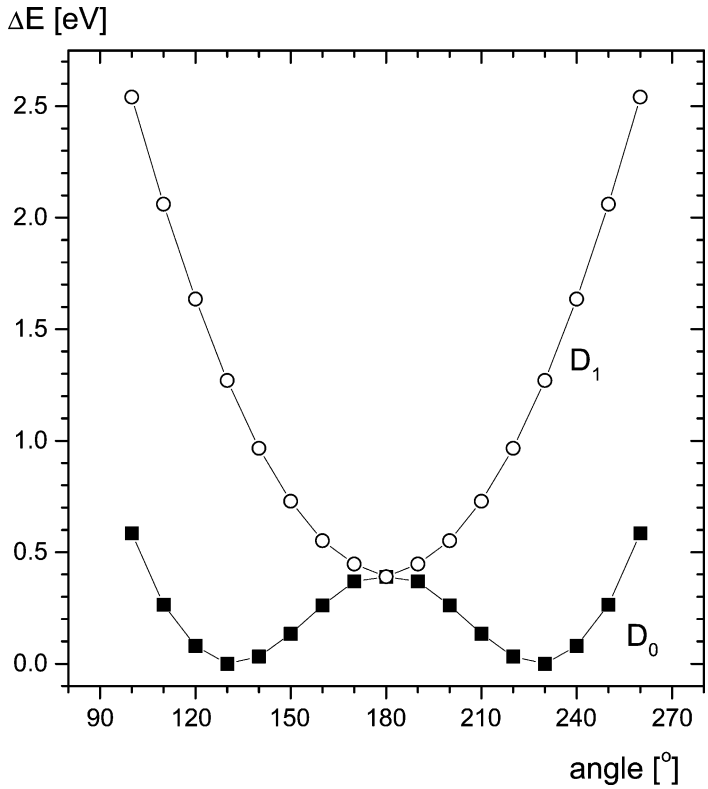

Fig. 4. Potential energy curves of D_0, D_1 states along the constrained bond angle.

located on chlorine lead to a rather small bonding angle of 95.0, 100.8, and 93.8° for iS_0, iT_1, and iT_2, respectively. The triplet excited states result from an excitation of a nonbonding electron on carbon, and thus, the geometry is not significantly influenced. The energy gap between the singlet ground state and the first triplet state (1.9 eV) is not as big as it is in H–C–Cl^{2+} (4.13 eV). Potential energy curves of the ground state iS_0 and of the excited states iT_1 and iT_2 (optimized structures) along the Cl–H bond distance are shown in Fig. 5. Further increase of the Cl–H bond length of the ground state iS_0 led to a rearrangement of C–Cl–H^{2+} to the H–C–Cl^{2+} dication. The transition state for rearrangement of the two isomers in the singlet state ($^1A'$), $iS_0 \rightarrow S_0$, has a Cl–H bond length of 2.286 Å, a C–Cl bond length of 1.623 Å, and a bond angle of 113.44°. The barrier height is 1.08 eV. The barrier for a rearrangement of C–Cl–H^{2+} in the triplet state iT_1 to H–C–Cl^{2+} in the triplet state T_1 is 1.19 eV. The transition state $^3A'$ is characterized by a Cl–H bond length of 1.550 Å, a C–Cl bond length of 1.623 Å, and by a bond angle of 57.85°. The characterization of the transition states was confirmed by finding the respective single imaginary frequency.

The corresponding cation C–Cl–H^+ was optimized in five electronic states ($iD_0\{^2A'\}$, $iD_1\{^2A''\}$, $iD_2\{^2A'\}$, $iD_3\{^2A''\}$, and $iQ_1\{^4A''\}$). The quartet $\{^4A'\}$ turned out to be dissociative. All calculated structures are bent. The electronic structures of the ground state iD_0 and of the first excited state iD_1 are similar to the orbital occupancy of the ground state of the dication, with one unpaired electron located on carbon. Therefore, the geometry is also similar.

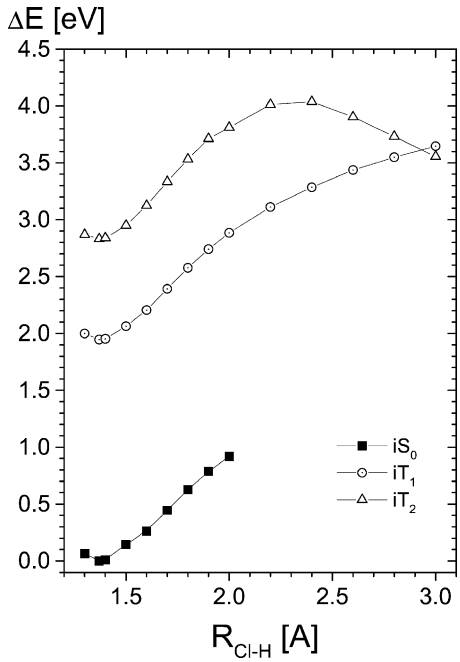

Fig. 5. Potential energy curves of iS_0, iT_1, iT_2 states along the constrained Cl–H bond. Further increasing of the Cl–H bond of C–Cl–H^{2+} in the ground state iS_0 leads to rearrangement of C–Cl–H^{2+} to H–C–Cl^{2+}.

3.3. Vertical charge transfer

For a direct comparison with charge transfer experiments

$$CHCl^{2+} + R \rightarrow CHCl^{+} + R^{+} \quad (R = \text{noble gas}) \tag{1}$$

vertical energies for the electron capture process were calculated (vertical recombination energies); i.e., the difference between the energy of dication in the optimized geometry and the energy of a cation in the same unrelaxed geometry. This assumption seems reasonable since the transfer of an electron proceeds faster than the geometry relaxation. All vertical recombination energies are summarized in Table 3(a) and (b).

For comparison, the corresponding adiabatic energies have been calculated as the difference of the total energies E_{tot} (in hartree, Table 2) of the dication and the corresponding cation in given states. In order to obtain adiabatic energies directly in electron volts values, it can be calculated as the difference of the relative energies E_{rel} of the dication and the corresponding cation in given states (Table 2).

Table 3
Vertical recombination energies (eV)

ΔE (eV)	$HCCl^+$					
	D_0	D_1	D_2	D_3	Q_1	Q_2
(a) RE($HCCl^+ \leftarrow HCCl^{2+}$)$_V$ $HCCl^{2+}$						
S_0	−16.78	−11.55	−10.54	−9.24	–	–
T_1	−21.06	−19.69	−17.08	−16.64	−17.46	−17.39
T_2	−21.15	−19.86	−17.55	−17.16	−17.91	−17.93
S_1	−21.31	−20.06	−17.83	−17.48	–	–
T_3	−21.39	−21.26	−17.67	−16.71	−17.49	−17.48
T_4	−21.50	−21.41	−18.14	−17.05	−17.78	−17.78
S_2	−21.49	−21.17	−17.86	−17.23	–	–
S_3	−21.35	−21.33	−18.34	−17.04	–	–
	$CClH^+$					
	iD_0	iD_1	iQ_1	iD_2	iD_3	
(b) RE($CClH^+ \leftarrow CClH^{2+}$)$_V$ $CClH^{2+}$						
iS_0	−17.81	−17.17	–	−13.42	−13.08	
iT_1	−19.59	−18.63	−17.58	−15.80	−15.17	
iT_2	−20.67	−20.09	−18.48	−16.21	−15.89	

Table 4
Vertical ionization energies (eV)

ΔE (eV), $HCCl^{2+}$	$HCCl^+$, X^2A'
(a) $IE(HCCl^+ \rightarrow HCCl^{2+})_V$	
S_0	18.25
T_1	21.80
T_2	22.52
S_1	22.89
T_3	23.24
T_4	23.65
S_2	23.50
S_3	*23.99*
$CClH^{2+}$	$CClH^+$, X^2A'
(b) $IE(CClH^+ \rightarrow CClH^{2+})_V$	
iS_0	18.01
iT_1	20.18
iT_2	20.84

Finally, to complete the picture, vertical energies of the opposite process, vertical ionization, i.e., the difference between energy of cation in the optimized geometry and the energy of dication in the same unrelaxed geometry, were calculated, too. All energies of the vertical ionization cation → dication are summarized in Table 4(a) and (b).

3.4. Comparison with experimental results

In this section, we apply the calculated energies of the isomers $CHCl^{2+}$ and $CHCl^+$ to the results of translational energy distributions obtained in studies of the charge transfer reaction

$$CHCl^{2+} + Ar \rightarrow CHCl^+ + Ar^+ \quad (2)$$

Only the lower ionization energy of Ar ($^2P_{3/2}$, 15.76 eV) of the spin-orbit doublet of Ar^+ will be considered in the following. The thermodynamic adiabatic exoergicity of the reaction, ΔE_A is

$$\Delta E_A = RE(M^+ \leftarrow M^{2+})_A - IE(Ar) \quad (3)$$

where $RE(M^+ \leftarrow M^{2+})_A$ is the dication–cation adiabatic recombination energy (adiabatic recombination energy $RE(M^+ \leftarrow M^{2+})_A$ is equal to the adiabatic ionization energy $IE(M^+ \rightarrow M^{2+})_A$). It can be calculated as the difference of E_{tot} (hartree) or E_{rel} (eV) of the dication and the corresponding cation (Table 2).

However, the position of the peaks in the translational energy spectrum corresponds much better to a vertical transition between the dication M^{2+} and the cation M^+ [31]. The vertical exoergicity is given as

$$\Delta E_A = RE(M^+ \leftarrow M^{2+})_V - IE(Ar) \quad (4)$$

where $RE(M^+ \leftarrow M^{2+})_V$ is the vertical recombination energy of M^{2+}. The vertical recombination energies of the $CHCl^{2+}$ dications are summarized in Table 3(a) and (b).

First, let us consider transitions in system H–C–Cl^{2+} → H–C–Cl^+. The vertical exoergicity ΔE_V for the transition from the ground state of H–C–Cl^{2+} S_0 to the ground state of its cation D_0 is 1.02 eV (ΔE_A = 1.55 eV). It lies below, the reaction window [32,33], which favors charge transfer processes with exoergicities from about 2–5 eV, thus, the charge transfer process involving the ground state of the $HCCl^{2+}$ dication should have a small cross-section. The difference between the energy of the vertical transition (1.02 eV) and the corresponding adiabatic transition (1.55 eV) will be mainly deposited in the deformation vibration (the changes in bond lengths are small), as it is connected with the change from the linear to the bent geometry. For the first triplet excited state T_1 only the vertical transition $T_1 \rightarrow D_1$ corresponds to some of the observed peaks (2.0, 2.9, and 3.8 eV). The calculated exoergicity ΔE_V is 3.93 eV (ΔE_A = 5.29 eV). The large difference between vertical and adiabatic energies (1.36 eV) is due to a large geometry change leading to a considerable vibrational excitation. For the second excited triplet state, T_2, the transition $T_2 \rightarrow D_1$ has an exoergicity of 4.1 eV (ΔE_A = 5.73 eV). This value is above the experimentally observed exoergicity and it is also connected with a large geometry change. Transitions to quartet states of the cation, $T_2 \rightarrow Q_1$ and $T_2 \rightarrow Q_2$, lead to exoergicities of 2.17 and 2.15 eV (ΔE_A = 2.26 and 2.22 eV), respectively, and thus, they fall into the region of the first observed peak (2.0 eV). The transition $S_1 \rightarrow D_2$ of the first

excited singlet state has an exoergicity of 2.07 eV ($\Delta E_A = 2.67$ eV) and lies also in the region of the first peak.

The transitions related to the isomer C–Cl–H^{2+} as a reactant lead to more satisfactory results when applied to the experimental results. The transition from the ground state of the dication to the ground state of the cation, $iS_0 \rightarrow iD_0$, leads to an exoergicity $\Delta E_V = 2.05$ eV ($\Delta E_A = 2.16$ eV) and fits well the first experimentally observed peak at 2.0 eV. The transitions from the first excited triplet state to the ground state of the cation iD_0 and to its first excited state iD_1, $iT_1 \rightarrow iD_0$, $iT_1 \rightarrow iD_1$, with exoergicities 3.83 and 2.87 eV ($\Delta E_A = 4.10$ and 3.67 eV) fit the two other observed peaks at 3.8 and 2.9 eV.

Thus, it appears that the translational energy spectrum of products of the reaction (1) can be explained by a reaction of the ground and excited states of the isomer dication C–Cl–H^{2+}. Translational energy spectra of products of reaction with Xe and Kr indicate that the reactant beam is a mixture of the two isomers, $HCCl^{2+}$ and $CClH^{2+}$. For a more detailed discussion of the experimental results, see ref. [22].

4. Conclusions

An extensive computational study on the ground and excited states of the $HCCl^{2+}$ dication (eight states calculated) and the $HCCl^{+}$ cation (six states calculated) was carried out. Adiabatic and vertical energies of transitions between all individual states of $HCCl^{2+}$ and $HCCl^{+}$ were calculated, however, the resulting energies did not provide a satisfactory explanation of the experimentally obtained translational energy spectra of products of charge transfer collisions with Ar, Kr, Xe, and D_2. This led to a conclusion that an isomer of $CHCl^{2+}$, $CClH^{2+}$, can participate in the charge transfer processes. Three states of $CClH^{2+}$ as well as five states of its cation were calculated. The transitions from the ground state and first excited state of $CClH^{2+}$ to the ground state and first excited state of its cation $CClH^{+}$ were shown to fit the experimental data very well.

Acknowledgements

Partial support of this research by the Grant Agency of the Czech Republic (Grant No. 203/00/0632), by the Grant No. 1AB4040302 of the Grant Agency of the Academy of Sciences, and by the Kontakt Project ME 561 of the Ministry of Education, Younth and Sports of the Czech Republic is gratefully acknowledged.

References

[1] F.H. Dorfman, J.D. Morrison, J. Chem. Phys. 35 (1961) 575.
[2] T. Ast, J.H. Beynon, R.G. Cooks, Org. Mass Spectrom. 7 (1972) 749.
[3] B.P. Mathur, E.M. Burgess, D.E. Bostwick, T.F. Moran, Org. Mass Spectrom. 17 (1982) 10.
[4] J.B. Fenn, N. Mann, C.K. Meng, S.F. Wong, Mass Spectrom. 9 (1990) 37.
[5] F. Maquin, D. Stahl, A. Sawaryn, P.R. von Schleyer, W. Koch, G. Frenkin, H. Schwarz, J. Chem. Soc., Chem. Commun. (1984) 504.
[6] M.W. Wong, B.F. Yates, R.H. Nobes, L.J. Radom, J. Am. Chem. Soc. 109 (1987) 1381, and earlier references cited therein.
[7] K. Lamertsma, P.R. von Schleyer, H. Schwarz, Angew. Chem. Int. Ed. Eng. 28 (1989) 1321.
[8] S.D. Price, M. Manning, S.R. Leone, J. Am. Chem. Soc. 116 (1994) 8673.
[9] Z. Dolejšek, M. Fárník, Z. Herman, Chem. Phys. Lett. 235 (1995) 99.
[10] Z. Herman, J. Žabka, Z. Dolejšek, M. Fárník, Int. J. Mass Spectrom. 192 (1999) 191.
[11] L. Mrázek, J. Žabka, Z. Dolejšek, J. Hrušák, Z. Herman, J. Phys. Chem. 104 (2000) 7294.
[12] K.A. Newson, S.D. Price, Chem. Phys. Lett. 294 (1998) 223.
[13] N. Tafadar, N. Kearney, S.D. Price, J. Chem. Phys. 115 (2001) 8819.
[14] P. Lablanquie, J. Delwiche, M.J. Hubinfranskin, I. Nenner, P. Morin, K. Ito, J.H.D. Eland, J.M. Robbe, G. Gandara, J. Fournier, P.G. Fournier, Phys. Rev. A 40 (1989) 5673.
[15] M. Hochlaf, F.R. Bennett, G. Chambaud, P. Rosmus, J. Phys. B: At. Mol. Opt. Phys. 31 (1998) 2163.
[16] J. Hrušák, Z. Herman, S. Iwata, Int. J. Mass Spectrom. 192 (1999) 165.
[17] J. Hrušák, Chem. Phys. Lett. 338 (2001) 189.
[18] J. Hrušák, Z. Herman, N. Sändig, W. Koch, Int. J. Mass Spectrom. 201 (2000) 269.
[19] J. Hrušák, N. Sändig, W. Koch, Int. J. Mass Spectrom. Ion Process. 187 (1999) 701.
[20] J. Roithová, J. Žabka, J. Hrušák, R. Thissen, Z. Herman, J. Phys. Chem. (submitted).
[21] J. Roithová, R. Thissen, J. Žabka, P. Franceschi, O. Dutuit, Z. Herman, Int. J. Mass Spectrom. 228 (2003) 487.

[22] J. Roithová, J. Žabka, J. Hrušák, Z. Herman, Phys. Chem. Chem. Phys. (submitted).
[23] D. Duflot, J.-M. Robbe, J.-P. Flament, Int. J. Mass Spectrom. Ion Process. 171 (1997) 215.
[24] R. Thissen, M. Simon, M.J. Hubin-Franskin, J. Chem. Phys. 101 (1994) 7548.
[25] P.G. Szalay, R.J. Bartlett, Chem. Phys. Lett. 214 (1993) 481.
[26] P. Nachtigall, J. Hrušák, O. Bludský, S. Iwata, Chem. Phys. Lett. 303 (1999) 441.
[27] H.-J. Werner, P.J. Knowles, J. Chem. Phys. 82 (1985) 5053.
[28] P.J. Knowles, H.-J. Werner, Chem. Phys. Lett. 115 (1985) 259.
[29] P.-O. Widmark, P.-A. Malmqvist, B.O. Roos, Theor. Chim. Acta 77 (1990) 291.
[30] MOLPRO is a package of ab initio programs written by H.-J. Werner, P.J. Knowles, with contributions from R.D. Amos, A. Bernhardsson, A. Berning, P. Celani, D.L. Cooper, M.J.O. Deegan, A.J. Dobbyn, F. Eckert, C. Hampel, G. Hetzer, T. Korona, R. Lindh, A.W. Lloyd, S.J. McNicholas, F.R. Manby, W. Meyer, M.E. Mura, A. Nicklass, P. Palmieri, R. Pitzer, G. Rauhut, M. Schütz, H. Stoll, A.J. Stone, R. Tarroni, T. Thorsteinsson.
[31] A. Ehbrecht, N. Mustafa, Ch. Ottinger, Z. Herman, J. Chem. Phys. 105 (1996) 9833.
[32] R.E. Olson, J. Chem. Phys. 56 (1972) 2976.
[33] K.G. Spears, F.C. Fehsenfeld, F. McFarland, E.E. Ferguson, J. Chem. Phys. 56 (1972) 2562.